Published in final edited form as:
Ann Biomed Eng. 2009 November ; 37(11): 2390–2401. doi:10.1007/s10439-009-9770-6.

In Vivo Demonstration of a Self-Sustaining, Implantable, Stimulated-Muscle-Powered Piezoelectric Generator Prototype

B. E. Lewandowski[1,2], **K. L. Kilgore**[2,3,4], and **K. J. Gustafson**[2,4]

[1] Bioscience and Technology Branch, NASA Glenn Research Center, 21000 Brookpark Rd., MS 110-3, Cleveland, OH 44135, USA

[2] Department of Biomedical Engineering, Case Western Reserve University, Cleveland, OH 44106-7207, USA

[3] Metro Health Medical Center, Cleveland, OH 44109, USA

[4] Louis Stokes Cleveland Department of Veterans Affairs Medical Center, Cleveland, OH 44106, USA

Abstract

An implantable, stimulated-muscle-powered piezoelectric active energy harvesting generator was previously designed to exploit the fact that the mechanical output power of muscle is substantially greater than the electrical power necessary to stimulate the muscle's motor nerve. We reduced to practice the concept by building a prototype generator and stimulator. We demonstrated its feasibility *in vivo*, using rabbit quadriceps to drive the generator. The generated power was sufficient for self-sustaining operation of the stimulator and additional harnessed power was dissipated through a load resistor. The prototype generator was developed and the power generating capabilities were tested with a mechanical muscle analog. *In vivo* generated power matched the mechanical muscle analog, verifying its usefulness as a test-bed for generator development. Generator output power was dependent on the muscle stimulation parameters. Simulations and *in vivo* testing demonstrated that for a fixed number of stimuli/minute, two stimuli applied at a high frequency generated greater power than single stimuli or tetanic contractions. Larger muscles and circuitry improvements are expected to increase available power. An implanted, self-replenishing power source has the potential to augment implanted battery or transcutaneously powered electronic medical devices.

Keywords

Piezoelectric energy conversion; Mechanical muscle power; Electrical stimulation; Rabbit

INTRODUCTION

Implanted electronic medical devices, such as pacemakers, deep brain stimulators, neurostimulators and intramuscular stimulators, are commonly used to provide beneficial therapies and increase quality of life.[2,3,5,14,24] However, power management of these devices remains a technical challenge. Power consuming devices such as neurostimulators use batteries implanted along with the device and require replacement surgeries when the batteries are depleted. Each surgery is costly and carries the common risks of surgical procedures.[6,27,53] Applications such as intramuscular stimulation have greater power requirements and may use

Address correspondence to B. E. Lewandowski, Bioscience and Technology Branch, NASA Glenn Research Center, 21000 Brookpark Rd., MS 110-3, Cleveland, OH 44135, USA. Beth.E.Lewandowski@nasa.gov.

transcutaneous power sources to provide high levels of energy transfer between external and internal coils or wires. The disadvantage of transcutaneous systems is the need for external equipment, which can be damaged, is burdensome to carry, is cosmetically unappealing and cannot be used in a wet environment. [39,43] A totally implantable electrical power source that is replenished by conversion of an energy source within the human body may be an advantageous alternative or augmentation to implanted batteries or transcutaneous power sources. The number of required battery replacement surgeries could be reduced or possibly eliminated. Periods of intramuscular device functionality untethered from external equipment could be possible, during which a shower or water therapy could be performed independently.

The concept of converting both external and internal human energy sources into electrical power has been studied for a variety of applications. For example, the thermal energy from surface body heat has been converted to electrical energy for powering wrist watches.[46] Human powered generators that convert mechanical energy to electricity include hand cranks for powering radios, shake generators for flashlights, cycle driven portable generators,[30] heel strike generators for lessening the weight burden that soldiers carry,[47] inductive and piezoelectric generators incorporated into hiking backpacks for powering mobile communication devices[12,44] and a regenerative brake located at the knee joint that operates using the negative work of locomotion for powering prosthetic limbs.[10] Research and development of implanted generators has included thermoelectric generators driven by body heat[34] and piezoelectric generators driven by bone strain,[11,42] acceleration during locomotion, [15] the motion of respiration[19] and heart contractions. [28,29] The power generated from these generators has been in the μW or sub-μW range and the potential applications have been small power consuming devices, such as telemetry of sensor data, drug pump delivery systems and pacemakers.

We have been developing a unique, implantable, active energy harvesting generator driven by stimulated skeletal muscle contractions. An advantage of skeletal muscle is that it contains a significant amount of potential chemical energy. A conservative estimate of the sustained mechanical output power of stimulated, conditioned skeletal muscle producing isotonic contractions is 1 mW/g.[1,18,50] The mass of human limb and trunk muscles range from 10 to 1000 g[41] and therefore the mechanical power available for conversion could be as great as 1 W. Active energy harvesting uses a small portion of the generated power to control the system in order to increase overall power transfer.[38] Our generator takes advantage of the fact that the μW's of electrical power necessary to stimulate a motor nerve is orders of magnitude less than the mW's of mechanical power available from muscle contractions or that can be harvested with piezoelectrics.[31] Motor nerve stimulation is used to drive muscle contractions in a constant and consistent pattern. We have chosen to use a piezoelectric stack to convert the mechanical power of the stimulated muscle into electrical power. The advantage of a piezoelectric stack is its small displacement, in the μm range. That limits the decrease in efficiency due to fibrous growth encapsulation and increases reliability by having no moving mechanical parts that could break.

The concept for the implantable, stimulated-muscle-powered piezoelectric generator is shown in Fig. 1. A piezoelectric stack generator in a mechanical holder is surgically attached between a bone and a muscle-tendon unit. A muscle that is paralyzed for which restoration of function is not anticipated or a redundant muscle whose function can be sacrificed are the types of muscles that are targeted to drive the generator. The motor nerve of the muscle is electrically stimulated to produce isometric muscle contractions, which repetitively exert force on the piezoelectric generator. As force is applied, the piezoelectric material is strained causing charge to develop, which is stored in electrical circuitry. A portion of the generated power is used to stimulate the motor nerve and the rest is available to power an implanted medical device application. Further details about the generator design have been previously reported in Lewandowski *et al.*[31,32]

Muscle force is the system parameter that has the largest effect on generator output power. The output power increases quadratically with increases in amplitude and linearly with increases in the frequency of the muscle force.[31] The amplitude of muscle force is dependent on the size of the muscle and the stimulation pattern (number of pulses, frequency and repetition rate) applied to the motor nerve.[7–9,17,23,40,55] Both muscle amplitude and frequency should be as large as possible for maximum output power. However, for sustained muscle activity without fatigue, there is a trade-off between smaller force muscle twitches repeated at a faster rate and larger force tetanic contractions repeated at a slower rate.

An additional condition for maximum power transfer is that the impedance of the load circuit needs to match the impedance of the generator. The impedance of the generator depends on the frequency of the muscle force. For un-fused contractions two frequencies are present, the un-fused stimulation frequency and the burst repetition rate. It is important to determine the frequency to which the load circuit should be tuned for maximum power transfer if multi-peak force bursts are used to drive the generator.

The goal of this study was to reduce to practice our concept of an implantable, self-sustaining stimulated-muscle-powered piezoelectric active energy harvesting generator that exploits the fact that the mechanical output power of a muscle is substantially greater than the electrical power necessary to stimulate the motor nerve. The study objectives were to (1) build a mechanical muscle analog to use as a test bed for generator development; (2) build a generator prototype consisting of a piezoelectric stack generator, storage circuitry, a motor nerve stimulator and a load resistor; (3) demonstrate continuous, self-sustaining operation of the stimulator and dissipation of additional power through the load resistor, *in vivo*, using rabbit quadriceps to drive the generator system; (4) verify the accuracy of the mechanical muscle analog by comparing data obtained with it to data obtained from *in vivo* trials; (5) determine the combination of stimulation parameters that results in maximum output power and determine the fundamental frequency to which the load circuit should be tuned.

METHODS

Mechanical Muscle Analog

A mechanical muscle analog test bed (Fig. 2) was built for generator prototype development and to reduce the number of required animal experiments. It was designed to produce tension with a magnitude and profile similar to that of a muscle twitch. This was achieved by using a linear motor controlled with an H-bridge circuit (TPIC0107B, Texas Instruments, Dallas, TX) to stretch and relax a spring. The spring was attached to the mechanical holder that housed the piezoelectric stack and converted tensile force to the compressive force needed for generator operation. The other end of the holder was anchored to the test stand. Tension (10–50 N) was controlled by the motor power supply voltage. Frequency (0.125–2 Hz) was controlled by the clock of the H-bridge circuit. Force was measured with a load cell (LC703-50, Omega Engineering, Inc., Stamford, CT).

The output power capabilities of the generator were assessed with the mechanical muscle analog. A 7 × 7 × 44 mm, modified lead zirconate titanate piezoelectric stack (TRS Technologies, State College, PA) with a piezoelectric constant of 0.035 V mN^{-1} and a capacitance of 323 nF was connected to the power analysis circuit (Fig. 3). The power analysis circuit consisted of a half diode bridge, a 1000 μF tantalum storage capacitor (C_L) and a 3 MΩ load resistor (R_{PA}), sized to match the impedance of the piezoelectric stack. The mechanical muscle analog was used to apply force ranging from 10 to 50 N to the piezoelectric stack in 18 trials until the voltage across R_{PA} reached a steady state (V_{Lss}). Data acquisition equipment (DAQPad 6052E & Labview Software, National Instruments, Austin, TX) was used

to acquire force and voltage data. The output power (P) was calculated with Eq. (1) and plotted vs. input force.

$$P = \frac{V_{Lss}^2}{R_{PA}} \tag{1}$$

Preparation for In Vivo Demonstration

A prototype generator system was specifically built for the *in vivo* demonstration. The prototype generator system consisted of the piezoelectric stack generator connected to a half diode bridge, a 1000 μF tantalum storage capacitor (C_L) a stimulator circuit and a load resistor (R_L) (Fig. 4). The load resistor R_L represented a target application and was used to measure the output power generated in addition to that needed for motor nerve stimulation. The simplified nerve stimulator was built from a CMOS Schmitt trigger circuit, producing a biphasic current pulse (using $C_2 = 0.2\ \mu$F) that was applied to the motor nerve through a custom fabricated tripolar spiral nerve cuff electrode. Potentiometer R_1 (100 kΩ potentiometer set at 5.6 kΩ) and capacitor C_1 (0.1 μF) controlled the pulse width of the stimulus, which could be adjusted to be between 10 and 2000 μs, and R_2 (100 MΩ) and C_1 (0.1 μF) controlled the inter pulse interval, which was set to approximately 1 s.

We chose to use the rabbit quadriceps muscle to drive the generator during the *in vivo* demonstration since simulations and mechanical testing of expected forces suggested this muscle would be sufficient. Estimates of output power expected from the generator when driven by rabbit quadriceps were compared to estimates of the power requirements of the stimulator to determine if there was adequate power for sustained operation of the stimulator. The rabbit quadriceps can produce 30–50 N of twitch force,[4,21,22,37] corresponding to 2–8 μW of output power, predicted from the simulation results of previous studies.[31] It was not possible to directly measure the stimulator power requirements since the measurement process changed the characteristics of the circuit, so an estimate was determined indirectly using the mechanical muscle analog. A 40 N force was applied with the mechanical muscle analog to the piezoelectric stack connected to the power analysis circuit (Fig. 3). A 2.4 V steady state voltage (V_{Lss}) resulted across R_{PA} (3 MΩ), corresponding to an output power of 1.9 μW, calculated with Eq. (1). The piezoelectric stack was then connected to the circuitry shown in Fig. 4, with the electrode-nerve impedance approximated with a 1 kΩ resistor. A 40 N force was applied with the mechanical muscle analog to the piezoelectric stack and load resistor R_L was adjusted until the steady state voltage was equal to the steady state voltage from the power analysis circuit trial (2.4 V). This occurred when R_L equaled 5 MΩ. The power requirement of the stimulator (P_{Stim}) was estimated to be 0.8 μW (Eq. 2), which is less than the predicted output power of the generator. The current pulse produced by the stimulator across the 1 kΩ resistor was a 700 μA, 200 μs pulse, a value that should be adequate for stimulating a motor nerve. These estimates provided confidence in the ability to demonstrate our generator *in vivo* using a rabbit quadriceps to drive the generator.

$$P_{Stim} = V_{Lss}^2 \left(\frac{1}{R_{PA}} - \frac{1}{R_L} \right) \tag{2}$$

In Vivo Experimental Protocol

Five New Zealand White rabbits (3.9 ± 0.4 kg, $n = 5$) were used in the study. The experimental protocol was approved by the Case Western Reserve University Institutional Animal Care and

Use Committee. Anesthesia was initiated with (50 mg/kg) Ketamine and (5 mg/kg) Xylazine and maintained throughout the experiment with 1–3% Isoflurane. A surgical procedure was performed to mechanically connect the piezoelectric generator to the rabbit quadriceps. The patellar tendon was detached from the tibia, keeping the muscle attachment to the tendon intact. A hole was drilled through the patella and connected to the piezoelectric holder with stainless steel wire. The other end of the piezoelectric holder was anchored to the test stand and the rabbit's ankle and knee joints were secured to prevent movement. A tripolar spiral nerve cuff electrode was placed on the femoral nerve. Stimulus parameters for maximal muscle activation were determined. The experimentation performed included (1) *in vivo*, self-sustaining demonstration of the generator concept; (2) *in vivo* power generation data collection for comparison to the mechanical muscle analog; (3) collection of *in vivo* force data for use in software simulations for the stimulation parameter study; and (4) *in vivo* power generation data collection for comparison to the software simulation results. The rabbits were euthanized at the conclusion of the experiment with a 90 mg/kg dose of sodium pentobarbital (Euthasol, Virbac AH, Inc., Fort Worth, TX), administered intravenously through the lateral ear vein. The animals were pronounced dead at cessation of heart beat and ECG readings, at which time the quadriceps muscle was dissected and weighed (63.8 ± 10 g, $n = 5$).

(1) In Vivo Self-Sustaining Demonstration of Generator Concept Feasibility—We demonstrated in one rabbit experiment that the mechanical power of muscle can be converted to electrical power in amounts greater than is needed for stimulation of the motor nerve. The ability of the generator to maintain a steady state or increase the output voltage during the *in vivo* trials demonstrated that our active energy harvesting generator concept was feasible. The capacitor C_L was pre-charged and resistor R_L was set to maintain a steady state voltage. Connection of the piezoelectric stack to the system circuit (Fig. 4) and connection of the nerve electrode to the stimulator initiated generator operation. The system was allowed to run for 120 s. The power generated in addition to that needed to power the stimulator was calculated with Eq. (1), using the value of R_L and the steady state voltage of the system.

(2) Comparison of In Vivo Data to Mechanical Analog Data—*In vivo* results were compared to results obtained with the mechanical muscle analog to verify its accuracy. The output power capability of the generator when driven by muscle was assessed in two *in vivo* experiments. The piezoelectric generator was mechanically connected to the muscle and electrically connected to the power analysis circuit (Fig. 3). Muscle length was adjusted to where maximum twitch force resulted and the minimum current level for producing maximum twitch forces was found. The femoral nerve was stimulated at 1 Hz (Pulsar Stimulators, FHC Inc., Bowdoinham, ME) until the voltage across the load resistor (V_L) reached a steady state. Capacitor (C_L) was pre-charged to decrease the time necessary for V_L to reach its steady state. The output power of the generator was calculated using Eq. (1) and the *in vivo* output power results were compared to the mechanical muscle analog output power data.

(3) In vivo Collection of Force Data for the Evaluation of Stimulus Parameters—A stimulation parameter study was performed to determine the combination of stimulation parameters that results in maximum output power and to determine whether the load circuit should be tuned to the stimulation frequency or the repetition rate frequency. The force of the rabbit quadriceps, resulting from the application of various stimulation patterns to the femoral nerve (Pulsar Stimulator, FHC Inc., Bowdoinham, ME), was recorded in three rabbit experiments. The stimulation patterns for a fixed aggregate rate of 1 stimuli/s were 1 pulse repeated at 1 Hz and trains of 2, 4, and 8 pulses at repetition rates of 0.5, 0.25, and 0.125, respectively. Stimulation frequencies for each of the trains of multiple pulses included 20, 40, 50, and 100 Hz. Three contractions were obtained during each trial of a stimulation pattern

combination and the force was averaged over those three contractions. At least two trials of each stimulation pattern were obtained.

Evaluation of Stimulus Parameters Using Software Simulations

In vivo muscle force data were used as input to software simulations which predicted the generator output power resulting from sustained application of each force waveform. The software simulation methods are described in detail in Lewandowski *et al.*[31] The SPICE circuit (EMA Design Automation, Inc., Rochester, NY) used in the simulations included a voltage source and capacitance to represent the piezoelectric stack, and a half diode bridge, storage capacitor and a load resistor. The piezoelectric voltage was calculated by multiplying the input force by a scalar, determined from the piezoelectric constant and dimensions of the piezoelectric stack. The output of the simulations was the steady state voltage (V_{Lss}) across the load resistor (R_L) and the predicted output power of the generator was calculated using Eq. (1).

For each input force trace, the output power was predicted over a range of load resistors (R_L = 10 kΩ to 1000 MΩ). The load resistor (R_{Lopt}) resulting in the greatest output power (P_{opt}) was determined. R_{Lopt} is related to the input impedance of the generator. Frequency (f_{sim}) was calculated with Eq. (3) using R_{Lopt} found in the software simulations and C_p = 323 nF. f_{sim} was compared to the stimulation frequency and the repetition rate of the stimulus to determine the frequency to which the load circuit should be tuned for maximum power transfer. Average peak force was defined as the peak force for twitches and the average of the peaks for un-fused contractions. The stimulation parameter combination (number of pulses in the train and stimulation frequency of the train) resulting in the greatest predicted output power was identified.

$$f_{sim}=\frac{1}{C_p R_{Lopt}} \tag{3}$$

(4) In Vivo Data Collection for Comparison with Software Simulation Predictions—A comparison of the output power of the generator using two different stimulation parameter combinations was performed during one rabbit experiment. The two stimulation parameter combinations were (1) single pulses repeated at 1 Hz; (2) the stimulation parameter combination predicted from the software simulations to result in the greatest output power. The piezoelectric generator was mechanically connected as described above and was electrically connected to the power analysis circuit, shown in Fig. 3. The load resistor (R_{PA}) was tuned according to the repetition rate. The two different stimulation parameters were applied (Pulsar Stimulator, FHC Inc., Bowdoinham, ME) until the voltage across the load resistor (V_L) reached a steady state. Capacitor C_L was pre-charged to decrease the time necessary for V_L to reach its steady state. The output power of the generator was calculated with Eq. (1) and compared for the two stimulation parameter combinations.

RESULTS

Output Power Capabilities of the Generator

The output power (P) of the generator as a function of applied force (F) when the mechanical muscle analog was used to apply force is shown in Fig. 5. The equation of the curve fitted through the data points was:

$$P=0.001F^2 - 0.0031F \qquad R^2=0.91 \tag{4}$$

A second order polynomial fit was chosen because the output power of the generator theoretically increases quadratically with the input force.[31] The shape of the fit through the mechanical analog data matches the shape of a fit through theoretical predictions performed with SPICE software simulations performed in a previous study.[31] The output power results from the mechanical analog experiments were a factor of 10 less than these theoretical output power predictions. The difference is due to mechanical coupling losses and electrical circuitry losses neglected in the simulations. The least-squares error method was used to fit the data to the second order polynomial. We assumed that the error (E) in the data was due to our inability to precisely measure the force produced by the mechanical muscle analog. We assumed it was independent normal with constant variance and that $P \pm 2E$ contained at least 90% of the predictions. The variation in force produced by the mechanical muscle analog within each trial was 2.1 ± 0.7 N (1.2–4.0 N).

In Vivo Demonstration of Generator Concept

In an *in vivo* experiment we demonstrated that the mechanical power of muscle can be converted to electrical power in amounts greater than is needed for stimulation of the motor nerve. Once the piezoelectric stack was mechanically connected to the rabbit quadriceps, operation of the generator system was initiated by connecting the piezoelectric stack to the system circuit and the femoral nerve electrode to the stimulator (Fig. 4). We used an initial condition of 100 MΩ for R_L and C_L was pre-charged to 1.65 V. From the mechanical analog experiments we observed that a significant portion of the generated power would be needed for operation of the stimulator when using force values of approximately 30 N. We expected that only a small amount of additional power would be generated, so we chose a large initial resistor value for R_L. Additionally, we observed a steady state system voltage of approximately 1.7 V when the mechanical muscle analog applied a 30 N force to the power analysis circuit. Therefore, we chose a voltage slightly below 1.7 V as the starting point for the *in vivo* trial.

The width of the current pulse generated by our stimulator during the *in vivo* demonstration was 1400 μs and the repetition rate was 0.6 Hz (Figs. 6a and 6b). A 500 μA, 200 μs pulse produced the same 30 N twitch with an external stimulator, therefore we estimate the current pulse amplitude from our stimulator to be 200 μA. Twitch force decreased over the 2 min run from 30 to 13 N. Figures 6c and 6d show example force twitches recorded at the end of the trial. We estimated for these force levels that the total power generated was between 0.1 and 1 μW (Fig. 5). Initial maximum twitch force was 35 N, thus the generator was operating at 37–86% of maximum twitch force. Each force pulse applied to the piezoelectric stack resulted in a step increase in the output voltage of the system (Figs. 6e and 6f). The step increases in voltage were greater at the beginning of the 120 s trial of continuous operation and leveled off at 1.7 V toward the end of the trial as the muscle fatigued (Fig. 7). During the period when the operating voltage was at 1.7 V, the generator produced an additional 30 nW of power through the 100 MΩ load resistor. Throughout the entire 120 s trial the generator produced continuous power for stimulator operation and additional power through the load resistor, demonstrating concept feasibility.

Comparison of In Vivo Data to Mechanical Analog Data

The output power generated during two *in vivo* trials matched the mechanical analog power results and was within 4% of the mechanical analog curve fit (Fig. 5). During one *in vivo* trial an average force of 11 N was produced by the quadriceps, the steady state voltage was 0.6 V

and the output power was 0.12 μW. Non-maximal force was obtained in this experiment, due to the abnormally high threshold current needed for this animal's femoral nerve. The other *in vivo* trial produced force in the expected range, 31 N, resulting in a steady state voltage of 1.7 V and an output power of 1 μW.

Stimulation Parameter Evaluation

When a multi-pulse stimulation pattern is applied to the motor nerve, the resulting muscle force waveform can contain two frequencies; the stimulation frequency and the repetition rate. The frequency to which the load circuit should be tuned for maximum power transfer was calculated for each of the stimulation parameter combinations with Eq. (3) using R_{Lopt} found from the software simulations (Table 1). Two cases were observed. In the first case the tuning frequency matched the repetition rate. This occurred for stimulation patterns that approached single force bursts: 1 Hz single pulses and multi-pulse trains with high stimulation frequencies (50 and 100 Hz and sometimes 40 Hz). In the second case, the tuning frequency was greater than the repetition rate but much less than the stimulation frequency and was approximately equal to the sum of the repetition rate and the number of pulses. This occurred for stimulation patterns of un-fused multi-pulse trains with a stimulation frequency of 20 Hz and sometimes 40 Hz. No advantage was obtained by tuning to the higher stimulation frequency as an averaging effect occurred between the stimulation frequency and the repetition rate for the un-fused, multi-pulse force profiles. When single force bursts are used the system should be tuned to the repetition rate to maximize power output.

The greatest predicted output power occurred when 2 stimulation pulses were applied with a stimulation frequency of 100 Hz and a repetition rate of 0.5 Hz (Table 2). The predicted output power was 4 times greater than the power obtained from muscle twitches. The variation in output power within a stimulus pattern group was due to pooled data from three rabbits. Since the repetition rate was chosen so that the power necessary for the stimulations was kept constant (a fixed number of 1 stimuli/s), the most advantageous stimulation pattern was the one with the greatest predicted output power.

In the *in vivo* trial the output power for 2 stimulation pulses at 100 Hz and a repetition rate of 0.5 Hz was 2.7 greater than the output power for 1 stimulus pulse repeated at 1 Hz. The 2 pulse stimulation pattern resulted in an average peak force of 83 N, a steady state voltage of 4 V and a continuous generator output power of 2.7 μW. The 1 pulse stimulation pattern resulted in an average peak force of 31 N, a steady state voltage of 1.7 V and a continuous generator output power of 1.0 μW.

DISCUSSION

We demonstrated in an acute animal model that the mechanical power available from an electrically stimulated muscle can be converted into electrical power in excess of that needed to power the motor nerve stimulator. To our knowledge this has not been demonstrated before. This approach takes advantage of the power amplification characteristics of muscle, where the mechanical output power of the muscle is much greater than the electrical power necessary to stimulate the motor nerve. In previous work we introduced the concept of a stimulated-muscle-powered piezoelectric generator.[31] In this study we reduced to practice our concept by building a generator and stimulator prototype and demonstrating its feasibility *in vivo*, using rabbit quadriceps to drive the generator. The generated power was sufficient for continuous self-sustaining operation of the stimulator and a small amount of additional power was dissipated through a load resistor (Fig. 7). This demonstration is the first step toward realizing a stimulated-muscle-powered generator that can be implanted within the human body and used as a power source for implanted medical devices.

The approximate power requirements of different types of implanted medical devices include: (1) 50 μW for small devices such as pacemakers and neurostimulators [6,54,56]; (2) 10 mW for intramuscular stimulation applications such as restoration of hand grasp[25]; and (3) 5 W for a ventricle assist device.[49] We anticipate that a small device application could be completely powered by our generator, if we use an estimate of 1 mW of net power from an improved generator version that is driven by a large human muscle. However, due to the need to sacrifice a muscle for implementation of the generator, the advantages of our generator may not outweigh the advantages of the battery technology that is currently used for these devices. The power requirement of the ventricle assist device is clearly outside the range of anticipated capabilities of our generator technology. Intramuscular stimulation applications, however, appear to be an appropriate target application for our generator. In this example, we would anticipate that the generator could supply 10% of the necessary power. We anticipate that further refinement of the system, as described in the following paragraphs, could conceivably enable the generator to supply 100% of the power necessary for intramuscular stimulation applications (approximately 10 mW).

The use of a larger muscle will have the largest impact toward increasing the output power of future generator prototypes. We used the smallest animal muscle possible for our *in vivo* demonstration resulting in μW's of total generated power and only 30 nW of power in excess of that needed to power the stimulator. An estimate of the range of twitch forces available from human muscle is 1–800 N,[13,35,36,41] assuming a conversion factor of 50 N cm^{-2},[16] and twitch force to be 10–30% of the maximal contractive force. The upper range of this twitch force is approximately 30 times greater than the twitch force of the rabbit (~30 N), increasing the expected output power of the generator by a factor of nearly 10^3, since output power increases quadratically with input force. This puts the output power of the generator in the mW range when using large human muscles, rather than in the μW range seen in these experiments. Since the input muscle stimulation power requirements remains essentially constant as muscle size increases, the generated power will increase as the size of the muscle increases.

Gains in generator output power may also be possible by using muscle shortening to optimize the muscle's mechanical power production if efficiency decreases due to fibrous growth interference can be overcome. Our generator system used a piezoelectric generator with no moving parts and μm displacements for reasons of reliability and efficiency. The mechanical power associated with a 23 μm displacement of a piezoelectric stack, using a 100 N, 0.25 s, 1 Hz triangular force pulses is 0.3 mW. A 60 N peak force and 2 cm displacement can produce a mechanical power of 0.15 W,[51] which is an increase of a factor of approximately 500. Therefore, it is worth exploring mechanical to electrical conversion devices that would operate with optimal muscle force and stroke. However, implanted devices that have relied on larger displacement to convert muscle power have experienced decreases in efficiency during chronic studies due to the interference of fibrous growth with generator motion,[28,29] so methods for minimizing the failure of moving parts and the reduced efficiency due to fibrous growth are critical aspects of the design.

Future versions of the generator should incorporate voltage regulation to optimize the power transfer between the piezoelectric generator and the load circuitry and to ensure that the stimulating pulse is the minimum pulse needed produce maximum twitch force. The current amplitude produced by our simplified low power stimulator was dependent on the operating voltage of the generator, which is not optimal. A long pulse width kept the current amplitude low, but used approximately three times more charge per pulse than needed for muscle activation. The steady state voltage that our system operated at produced a current pulse which generated 37–83% of maximal twitch force. A fixed input voltage for the stimulator would result in a constant stimulus current and would prevent wasted energy. This could be achieved by adding a DC–DC converter commonly used with piezoelectric generators[26,42,48] to the

system to regulate the voltages of the stimulator and the load. Additionally, emerging technologies should be incorporated [33] into the design of the stimulator and the electrical circuitry should be customized to further reduce power costs.

This study took the first steps toward identifying the muscle stimulation parameters that are the most advantageous for generating output power for this application. The output power of the piezoelectric generator increases as both the magnitude and frequency of the applied force increase. However, the muscle force dynamics are complicated by the trade-off between force amplitude and contraction rate. The data demonstrate that repetition rate was the dominant frequency for tuning the system to maximize power output (Table 1) and that no advantage could be achieved by tuning the circuit to the stimulation frequency seen in non-fused contractions. When using repetition rates that keep the stimulating power requirements constant, the use of two high frequency stimulus pulses out performed the use of single pulses and of 4 and 8 pulse trains by generating three to four times as much output power (Table 2 and *in vivo* results). Two pulses per burst can optimize the force per pulse.[7–9,17,23,40,55] The force produced by the two pulses was much greater than the force produced by twitches and only slightly less than the force produced with 4 and 8 pulses. However, the two pulse stimulus trains can be applied at a higher repetition rate than 4 or 8 pulse trains.

Additional studies are necessary to fully understand the potential benefit of the use of two high frequency stimulus pulses. To implement the use of multi-pulse stimulus trains an additional timer would be required, adding power costs to the stimulator circuit. Chronic low frequency stimulation conditions muscle, resulting in a slower, fatigue resistant fiber type population,[20] which produces less maximal force than fast twitch type fiber.[45] Therefore, the potential gain in power could be used up in additional stimulator power costs and the effectiveness of a two pulse, high frequency stimulus train may be reduced in slower muscles. The simulation tools developed in this study can aid investigations of this type that weigh the benefits with the disadvantages.

A mechanical muscle analog was built to aid in the development of the prototype generator built for this study. Comparison of mechanical muscle analog data and *in vivo* data from this study verified its accuracy (Fig. 5). The mechanical muscle analog is a tool that can be used during the development of future generator prototypes. Chronic animal studies are needed to study attachment strategies,[52] biocompatibility and demonstrate chronic device performance.

CONCLUSION

This study demonstrated that the mechanical power from muscle contractions can be converted to electrical power in excess of that needed to stimulate the motor nerve of the muscle. We reduced to practice our concept by building a generator and stimulator prototype and demonstrating its feasibility *in vivo*, using a rabbit quadriceps to drive the generator. The generated power was sufficient for continuous operation of the stimulator and a small amount of additional power was dissipated through a load resistor. In addition, a mechanical muscle analog was built and its usefulness as a test-bed for future generator developments was verified. More complex stimulation patterns that may increase the output power capabilities in future versions of the generator were identified. An implantable, stimulated-muscle-powered generator system has the potential to be a power source for implanted electronic medical devices.

Acknowledgments

This project was funded by NASA Glenn Research Center's Human Health and Performance Project, The State of Ohio BRTT 03-10, the Department of Veterans Affairs RR&D B367R, the NIH DK077089 and supported by the Cleveland Functional Electrical Stimulation Center. We would like to acknowledge the contribution of Narendra

Bhadra, CWRU, who designed the nerve cuff electrodes used in the animal experiments. We would like to acknowledge the contributions of Fred Montague, CWRU, who designed the low power stimulator and Steve Garverick, CWRU, who provided design advice on the load circuitry used in our system.

References

1. Araki K, Nakatani T, Toda K, Taenaka Y, Tatsumi E, Masuzawa T, Baba Y, Yagura A, Wakisaka Y, Eya K, et al. Power of the fatigue resistant in situ latissimus dorsi muscle. ASAIO J 1995;41:M768–M771. [PubMed: 8573910]
2. Bhadra N, Kilgore KL, Peckham PH. Implanted stimulators for restoration of function in spinal cord injury. Med Eng Phys 2001;23:19–28. [PubMed: 11344004]
3. Bhadra N, Peckham PH. Peripheral nerve stimulation for restoration of motor function. J Clin Neurophysiol 1997;14:378–393. [PubMed: 9415385]
4. Burton HW, Stevenson TR, White TP, Hartman J, Faulkner JA. Force deficit of vascularized skeletal muscle grafts in rabbits. J Appl Physiol 1989;66:675–679. [PubMed: 2708198]
5. Creasey GH. Electrical stimulation of sacral roots for micturition after spinal cord injury. Urol Clin North Am 1993;20:505–515. [PubMed: 8351775]
6. Deharo JC, Djiane P. Pacemaker longevity. Replacement of the device. Ann Cardiol Angeiol (Paris) 2005;54:26–31. [PubMed: 15702908]
7. Ding J, Chou LW, Kesar TM, Lee SC, Johnston TE, Wexler AS, Binder-Macleod SA. Mathematical model that predicts the force-intensity and force-frequency relationships after spinal cord injuries. Muscle Nerve 2007;36:214–222. [PubMed: 17503498]
8. Ding J, Lee SC, Johnston TE, Wexler AS, Scott WB, Binder-Macleod SA. Mathematical model that predicts isometric muscle forces for individuals with spinal cord injuries. Muscle Nerve 2005;31:702–712. [PubMed: 15742371]
9. Ding J, Wexler AS, Binder-Macleod SA. A predictive model of fatigue in human skeletal muscles. J Appl Physiol 2000;89:1322–1332. [PubMed: 11007565]
10. Donelan JM, Li Q, Naing V, Hoffer JA, Weber DJ, Kuo AD. Biomechanical energy harvesting: Generating electricity during walking with minimal user effort. Science 2008;319:807–810. [PubMed: 18258914]
11. Elvin N, Elvin AA, Spector M. A self-powered mechancial strain energy sensor. Smart Mater Struct 2001;10:293–299.
12. Feenstra J, Granstrom J, Sodano H. Energy harvesting through a backpack employing a mechanically amplified piezoelectric stack. Mech Syst Signal Process 2008;22:721–734.
13. Fukunaga T, Roy RR, Shellock FG, Hodgson JA, Day MK, Lee PL, Kwong-Fu H, Edgerton VR. Physiological cross-sectional area of human leg muscles based on magnetic resonance imaging. J Orthop Res 1992;10:928–934. [PubMed: 1403308]
14. Glenn WW, Phelps ML, Elefteriades JA, Dentz B, Hogan JF. Twenty years of experience in phrenic nerve stimulation to pace the diaphragm. Pacing Clin Electrophysiol 1986;9:780–784. [PubMed: 2432480]
15. Goto H, Sugiura T, Harada Y, Kazui T. Feasibility of using the automatic generating system for quartz watches as a leadless pacemaker power source. Med Biol Eng Comput 1999;37:377–380. [PubMed: 10505390]
16. Granata KP, Marras WS. An EMG-assisted model of trunk loading during free-dynamic lifting. J Biomech 1995;28:1309–1317. [PubMed: 8522544]
17. Griffin L, Godfrey S, Thomas CK. Stimulation pattern that maximizes force in paralyzed and control whole thenar muscles. J Neurophysiol 2002;87:2271–2278. [PubMed: 11976366]
18. Gustafson KJ, Marinache SM, Egrie GD, Reichenbach SH. Models of metabolic utilization predict limiting conditions for sustained power from conditioned skeletal muscle. Ann Biomed Eng 2006;34:790–798. [PubMed: 16598656]
19. Hausler, E.; Stein, L. Implantable physiological power supply with PVDF film. In: Galletti, PM.; De Rossi, DE.; De Reggi, AS., editors. Medical Applications of Piezoelectric Polymers. New York, NY: Gordon and Breach Science Publishers; 1988. p. 259-264.

20. Jarvis JC. Power production and working capacity of rabbit tibialis anterior muscles after chronic electrical stimulation at 10 Hz. J Physiol 1993;470:157–169. [PubMed: 8308723]
21. Kaab MJ, Ito K, Clark JM, Notzli HP. Deformation of articular cartilage collagen structure under static and cyclic loading. J Orthop Res 1998;16:743–751. [PubMed: 9877400]
22. Kaab MJ, Ito K, Rahn B, Clark JM, Notzli HP. Effect of mechanical load on articular cartilage collagen structure: a scanning electron-microscopic study. Cells Tissues Organs 2000;167:106–120. [PubMed: 10971035]
23. Karu ZZ, Durfee WK, Barzilai AM. Reducing muscle fatigue in FES applications by stimulating with N-let pulse trains. IEEE Trans Biomed Eng 1995;42:809–817. [PubMed: 7642195]
24. Keith MW, Peckham PH, Thrope GB, Stroh KC, Smith B, Buckett JR, Kilgore KL, Jatich JW. Implantable functional neuromuscular stimulation in the tetraplegic hand. J Hand Surg [Am] 1989;14:524–530.
25. Kilgore, KL. Personal Communication: Power consumption of a hand grasp neuroprosthesis. 2003.
26. Kim H, Priya S, Stephanou H, Uchino K. Consideration of impedance matching techniques for efficient piezoelectric energy harvesting. IIEEE Trans Ultrason Ferroelectr Freq Control 2007;54:1851–1859.
27. Kindermann M, Schwaab B, Berg M, Frohlig G. Longevity of dual chamber pacemakers: device and patient related determinants. Pacing Clin Electrophysiol 2001;24:810–815. [PubMed: 11388100]
28. Ko, WH. 19th Annual Conference of the Society for Engineering in Medicine and Biology. 1966. Piezoelectric energy converter for electronic implants; p. 67
29. Ko, WH. Power sources for implant telemetry and stimulation systems. In: Amlaner, CJ.; MacDonald, D., editors. A Handbook on Biotelemetry and Radio Tracking. Elmsford, NY: Pergamon Press, Inc; 1980. p. 225-245.
30. Krikke J. Sunrise for energy harvesting products. IEEE Pervasive Comput 2005;4:4–8.
31. Lewandowski BE, Kilgore KL, Gustafson KJ. Design considerations for an implantable, muscle powered piezoelectric system for generating electrical power. Ann Biomed Eng 2007;35:631–641. [PubMed: 17295066]
32. Lewandowski, BE.; Kilgore, KL.; Gustafson, KJ. Energy Harvesting Technologies. In: Priya, S.; Inman, DJ., editors. Feasibility of an implantable, stimulated muscle-powered piezoelectric generator as a power source for implanted medical devices. New York, NY: Springer Science + Business Media, LLC; 2009. p. 389-404.
33. Lin, Y.; Sylvester, D.; Blaauw, D. IEEE Custom Integrated Circuits Conference. San Jose, CA: 2007. A sub-pW timer using gate leakage for ultra low-power sub-Hz monitoring systems.
34. MacDonald, SG. Biothermal power source for implantable devices. US Patent. 6,640,137. Oct 28. 2003
35. Marras WS, Jorgensen MJ, Granata KP, Wiand B. Female and male trunk geometry: size and prediction of the spine loading trunk muscles derived from MRI. Clin Biomech (Bristol, Avon) 2001;16:38–46.
36. Maurel, W. Dissertation. Ecole Polytechnique Federale de Lausanne; 1998. 3D Modeling of the Human Upper Limb Including the Biomechancis of Joints, Muscles and Soft Tissues.
37. Notzli H, Clark J. Deformation of loaded articular cartilage prepared for scanning electron microscopy with rapid freezing and freeze-substitution fixation. J Orthop Res 1997;15:76–86. [PubMed: 9066530]
38. Ottman GK, Hofmann HF, Bhatt AC, Lesieutre GA. Adaptive piezoelectric energy harvesting circuit for wireless remote power supply. IEEE Trans Power Electron 2002;17:669–676.
39. Ozeki T, Chinzei T, Abe Y, Saito I, Isoyama T, Mochizuki S, Ishimaru M, Takiura K, Baba A, Toyama T, Imachi K. Functions for detecting malposition of transcutaneous energy transmission coils. ASAIO J 2003;49:469–474. [PubMed: 12918593]
40. Parmiggiani F, Stein RB. Nonlinear summation of contractions in cat muscles. II. Later facilitation and stiffness changes. J Gen Physiol 1981;78:295–311. [PubMed: 7328404]
41. Pierrynowski, MR. Analytic representation of muscle line of action and geometry. In: Allard, P.; Stokes, IAF.; Blanchi, JP., editors. Three-Dimensional Analysis of Human Movement. Champaign, IL: Human Kinetics; 1995. p. 215-256.

42. Platt SR, Farritor S, Haider H. On low-frequency electric power generation with PZT ceramics. IEEE/ASME Trans Mechatronics 2005;10:240–252.
43. Puers R, Vandevoorde G. Recent progress on transcutaneous energy transfer for total artificial heart systems. Artif Organs 2001;25:400–405. [PubMed: 11403672]
44. Rome LC, Flynn L, Goldman EM, Yoo TD. Generating electricity while walking with loads. Science 2005;309:1725–1728. [PubMed: 16151012]
45. Salmons S, Vrbova G. The influence of activity on some contractile characteristics of mammalian fast and slow muscles. J Physiol 1969;201:535–549. [PubMed: 5767881]
46. Seiko Watch Company. Seiko World's First. 2009. http://www.seikowatches.com/heritage/worlds_first.html [Online]
47. Shenck NS, Paradiso JA. Energy scavenging with shoe-mounted piezoelectrics. IEEE Micro 2001;21:30–42.
48. Tan, YK.; Hoe, KY.; Panda, SK. Energy harvesting using piezoelectric igniter for self-powered radio frequency (RF) wireless sensors. IEEE International Conference on Industrial Technology; Mumbai, India. 2006.
49. Trumble, DR. Personal Communication: Power requirements of VAD. 2009.
50. Trumble DR, LaFramboise WA, Duan C, Magovern JA. Functional properties of conditioned skeletal muscle: implications for muscle-powered cardiac assist. Am J Physiol 1997;273:C588–C597. [PubMed: 9277356]
51. Trumble DR, Melvin DB, Dean DA, Magovern JA. In vivo performance of a muscle-powered drive system for implantable blood pumps. ASAIO J 2008;54:227–232. [PubMed: 18496270]
52. Trumble DR, Melvin DB, Magovern JA. Method for anchoring biomechanical implants to muscle tendon and chest wall. ASAIO J 2002;48:62–70. [PubMed: 11814099]
53. Vorperian VR, Lawrence S, Chlebowski K. Replacing abdominally implanted defibrillators: effect of procedure setting on cost. Pacing Clin Electrophysiol 1999;22:698–705. [PubMed: 10353127]
54. Wenzel, B. Dissertation. Case Western Reserve University; 2005. Closed-loop Electrical Control of Urinary Continence.
55. Wexler AS, Ding J, Binder-Macleod SA. A mathematical model that predicts skeletal muscle force. IEEE Trans Biomed Eng 1997;44:337–348. [PubMed: 9125818]
56. Wong LSY, Hossain S, Ta A, Edvinsson J, Rivas DH, Naas H. A very low-power CMOS mixed-signal IC for implantable pacemaker applications. IEEE J Solid-State Circuit 2004;39:2446–2456.

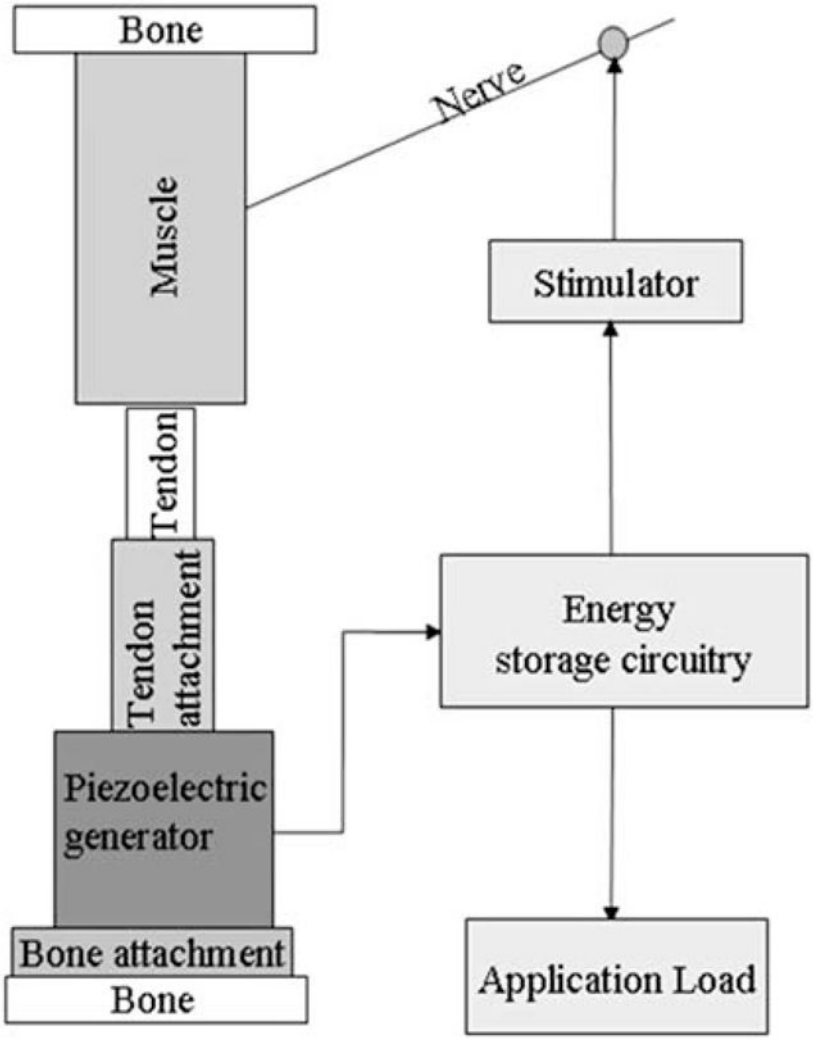

FIGURE 1.

The implantable, stimulated-muscle-powered piezoelectric energy generator concept. A piezoelectric stack generator in a mechanical holder is surgically attached between a bone and muscle-tendon unit. Stimulation of the motor nerve causes isometric muscle contractions, repetitively exerting force on the piezoelectric generator. The charge developed by the strained piezoelectric material is stored in electrical circuitry. A portion of the generated power is used to power the stimulator and the rest is available to power an implanted medical device application.

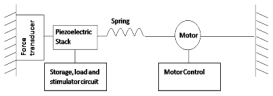

FIGURE 2.

Schematic of the mechanical muscle analog test bed. The mechanical muscle analog was used to develop and test the generator system prior to *in vivo* trials, reducing the number of animal experiments. The linear motor, controlled with an H-bridge circuit, stretched and relaxed a spring to produce tension with a magnitude and profile similar to that of a muscle twitch. The available force (10–50 N) was controlled with the motor power supply voltage. The clock of the H-bridge circuit was used to control the frequency of the force pulses.

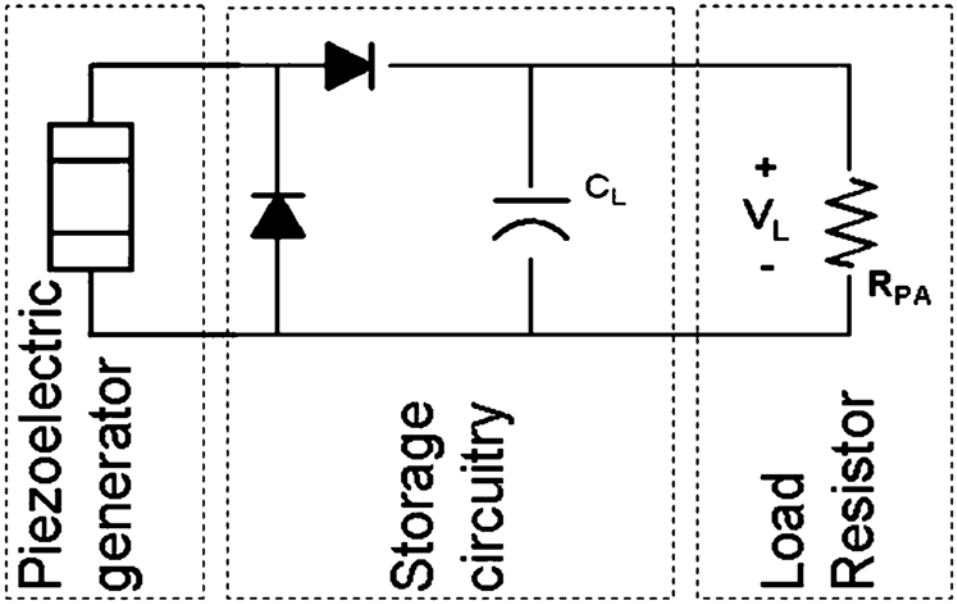

FIGURE 3.

Power analysis circuit schematic. The electrical schematic of the system used to measure the power generating capabilities of the implantable, stimulated-muscle-powered piezoelectric generator concept. The storage circuit consisted of a half diode bridge and a 1000 μF capacitor (C_L). The load resistor (R_{PA}) was matched to the impedance of the piezoelectric generator. Voltage (V_L) was recorded across the load resistor and power was calculated using Eq. (1).

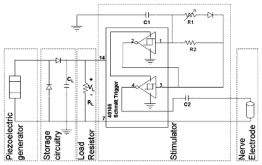

FIGURE 4.

Generator system circuit schematic. The electrical schematic of the system built to demonstrate the implantable, stimulated-muscle-powered piezoelectric generator concept. Stimulated muscle contractions applied force to the piezoelectric generator which powered both the stimulator and a load. The stimulator delivered a current pulse to the motor nerve which produced muscle contractions.

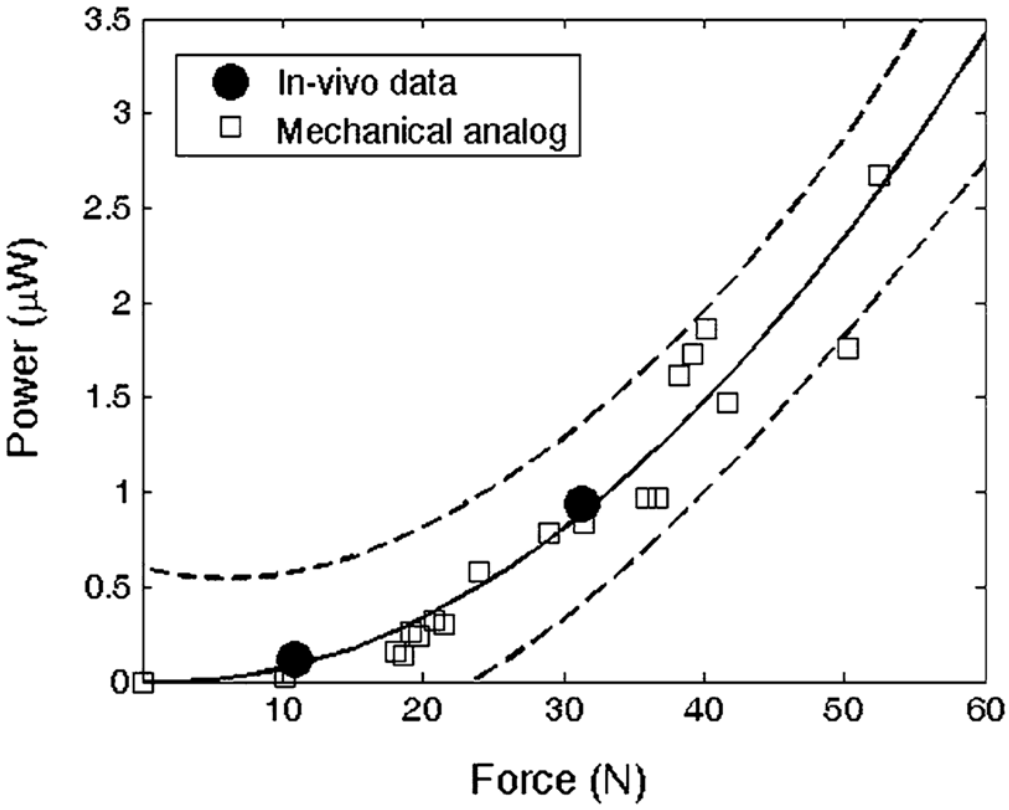

FIGURE 5.

In vivo power generation matched the mechanical muscle analog. The output power of the generator is shown as a function of input force applied with both the mechanical muscle analog (white squares) and the two *in vivo* experiments (black circles). The variation in force within each trial is contained within the markers. The solid line is a polynomial curve fitted through the mechanical analog data points. The dashed lines show the 90% confidence interval of the mechanical muscle analog data points.

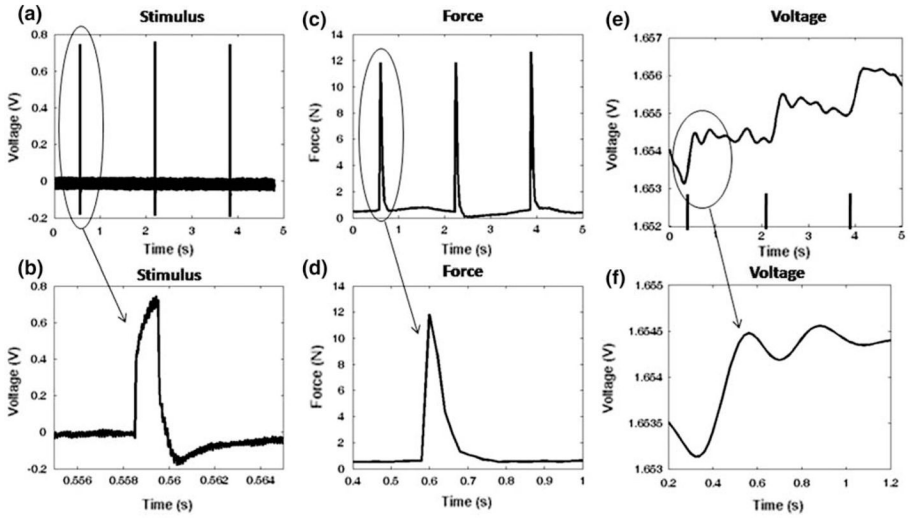

FIGURE 6.

Example stimulus pulse, twitch force and step increases in output voltage during the *in vivo* demonstration. Application of the stimulating pulses (a and b) to the rabbit femoral nerve resulted in quadriceps twitch force (c and d). The twitch force was applied to the piezoelectric stack resulting in a step increase in generator output voltage (V_L) (e and f). Continuous application of the stimulus pulses and resulting force bursts resulted in the self-sustaining generator operating voltage charging shown in Fig. 7.

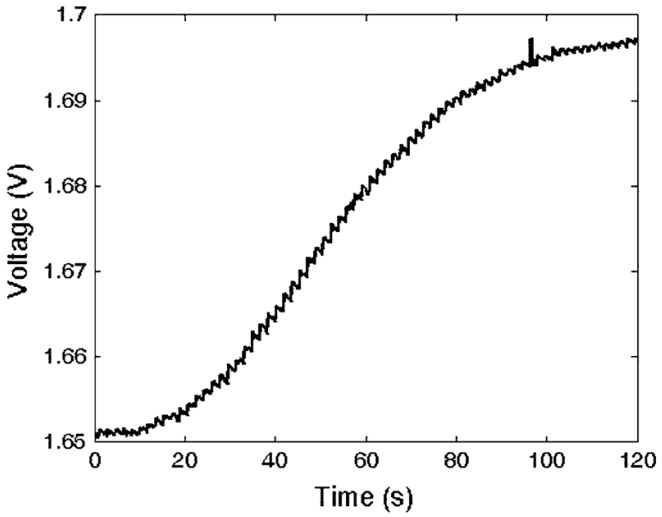

FIGURE 7.

Self-sustaining, *in vivo* power generation. This is the recorded output voltage (V_L) when the rabbit quadriceps was driving the generator system shown in Fig. 4. The generator charges C_L to a steady state voltage producing continuous power in an amount sufficient to run the stimulator and to dissipate 30 nW of additional power through a 100 MΩ load resistor. The ability of the generator to increase the output voltage of the system and to maintain a steady state demonstrates the feasibility of our generator concept.

TABLE 1

The load circuit tuning frequency for stimulation pattern combinations.

Number of pulses	Stimulation frequency (Hz)	Repetition rate (Hz)	Tuning frequency Mean ± SD (Hz)
Case 1: Tuning frequency matched repetition rate			
1	N/A	1	1.0 ± 0.0
2	40	0.5	0.5 ± 0.0
2	50	0.5	0.5 ± 0.0
2	100	0.5	0.5 ± 0.0
4	50	0.25	0.25 ± 0.0
4	100	0.25	0.25 ± 0.0
8	50	0.125	0.2 ± 0.1
8	100	0.125	0.125 ± 0.0
Case 2: Tuning frequency did not match repetition rate or stimulation frequency			
2	20	0.5	1.0 ± 0.0
4	20	0.25	0.7 ± 0.1
4	40	0.25	0.6 ± 0.25
8	20	0.125	1.0 ± 0.0
8	40	0.125	0.7 ± 0.5

Note: For single pulses of force the tuning frequency matched the repetition rate. For un-fused multi-pulse force bursts, the tuning frequency was greater than the repetition rate and substantially lower than the stimulation frequency. Therefore the system should be tuned to the repetition rate to maximize power output.

TABLE 2

Predicted output power for different stimulation patterns.

Power (μW) Mean ± SD	Force (N) Mean ± SD	Number of pulses	Stimulation frequency (Hz)	Repetition rate (Hz)
44.12 ± 8.97	77.86 ± 7.86	2	100	0.5
35.24 ± 6.84	54.74 ± 5.09	2	50	0.5
24.6 ± 8.27	81 ± 14.72	4	100	0.25
20.78 ± 0.76	44.01 ± 4.1	2	40	0.5
18.1 ± 1.57	54.97 ± 5.03	4	50	0.25
16.11 ± 0.61	93.61 ± 2.7	8	100	0.125
15.69 ± 0.43	38.54 ± 1.82	8	20	0.125
14.98 ± 5.97	33.22 ± 5.83	2	20	0.5
14.27 ± 3.92	56.47 ± 8.04	8	40	0.125
13.68 ± 7.92	34.69 ± 5.55	4	20	0.25
13.65 ± 7.03	44.5 ± 10.3	4	40	0.25
11.16 ± 10.7	24.95 ± 13.02	1	N/A	1
10 ± 2.28	56.68 ± 4.15	8	50	0.125

Note: The patterns consisted of different combinations of the number of stimulus pulses, the stimulation frequency and the repetition rate. For a fixed number of 1 stimuli/s, two stimuli applied at a high frequency generated greater power than single twitches or tetanic contractions.